

# Determination of the longitudinal scattering fraction in $pp \rightarrow W^\pm W^\pm jj$ using a deep machine learning technique

( Dated: July 7, 2015)

The unitarization of the longitudinal vector boson scattering (VBS) cross section by the Higgs boson is a fundamental prediction of the Standard Model which has not been experimentally verified. In the first LHC run, both the ATLAS and CMS collaborations presented first studies of VBS processes in events with two leptonically-decaying same-electric-charge  $W$  bosons produced in association with two jets. This channel has the advantage of smaller backgrounds compared to other VBS channels while still exhibiting a detectable production rate. However, the angular distributions of the leptons in the  $W$  boson rest frame, which are commonly used to fit polarization fractions, are not readily available in this process due to the presence of two neutrinos in the final state. In this paper we present a method to circumvent this problem by using a deep machine learning technique to recover these angular distributions from measurable event kinematics to determine the longitudinal scattering fraction. We compare the results obtained from this method with other traditional methods. The method presented here can be used as well in other VBS channels with neutrino(s) in the final state.

PACS numbers: 14.70m

## I. INTRODUCTION

The discovery of a Higgs-like boson at the LHC [1, 2] was the first step toward a better understanding of the electroweak symmetry breaking (EWSB) mechanism. One important, and unverified, prediction of the Standard Model (SM) is that the scattering amplitude of longitudinal vector bosons ( $V_L V_L \rightarrow V_L V_L$ ) is unitarized by the Higgs boson. Measuring VBS processes at a hadron collider, however, is experimentally challenging. The ATLAS and CMS collaborations recently provided the first evidence for and study of a VBS process using events with two same-electric-charge  $W$  bosons in association with two forward jets ( $pp \rightarrow W^\pm W^\pm jj$ ) [3, 4]. This final state has the advantage of relatively small SM background contributions compared to other VBS processes, paired with a production rate large enough to measure in early LHC datasets. While an ideal candidate for first observation of the VBS process, measuring the longitudinal fraction of these events is not straight forward.

In general the polarization of a gauge boson can be determined from the angular distribution of its decay products. Since a  $W$  boson only couples to left-handed particles and right-handed anti-particles. In the rest frame of the  $W$  boson, the decayed charged lepton is expected to preferentially pointing in the  $W$  boson spin direction for  $W^+$  and in the opposite  $W$  boson spin direction for  $W^-$ . **Two sentences are disconnected - what are you trying to say? Preferred emission depends on  $W$  helicity states...** The normalized differential cross section of a leptonically-decaying  $W$  boson can be written in terms of polarization fractions as [? ]:

$$\frac{1}{\sigma} \frac{d\sigma}{d\cos\theta^*} = \frac{3}{8} f_- (1 \mp \cos\theta^*)^2 + \frac{3}{8} f_+ (1 \pm \cos\theta^*)^2 + \frac{3}{4} f_L (1 - \cos^2\theta^*), \text{ for } W^\pm \quad (1)$$

where  $\theta^*$  is the angle between the charged lepton in the  $W$  boson rest frame and the  $W$  boson direction of motion.

The three fraction parameters  $f_-$ ,  $f_+$  and  $f_L$  denote the fractions of  $W$  events with three possible helicity states  $-1$ ,  $+1$  and  $0$ , respectively. They are constrained via  $f_- + f_+ + f_L = 1$ . In order to measure  $\theta^*$ , we need to fully reconstruct the direction of motion of the  $W$  boson.

Requiring both  $W$  bosons to decay leptonically in the  $pp \rightarrow W^\pm W^\pm jj$  events enables the determination of the charge of each  $W$  boson via the charged leptons. However, since the corresponding two neutrinos in the final state escape detection, the  $W$  boson rest frames cannot be directly measured. It is thus difficult to determine the polarization fractions of each boson and the fraction of longitudinal scattering events in the  $W^\pm W^\pm jj$  process.

Many proposals have been made to determine the longitudinal scattering fractions in other VBS final states, such as semi-leptonic  $WW$  [5] **How does the hadronic  $W$  charge assignment work?**,  $WZ$  [? ] and  $ZZ$  [? ] or fully-leptonic decay modes of  $WZ$  and  $ZZ$  scattering, where the full event kinematics can be reconstructed. However, these channels either suffer from large SM backgrounds not present in the  $W^\pm W^\pm jj$  channel or have relatively low production cross sections. Attempts have been made to gain sensitivity through other variables than  $\theta^*$  in the  $W^\pm W^\pm jj$  channel. One example is the variable  $R_{p_T} = (p_T^{\ell_1} \times p_T^{\ell_2}) / (p_T^{j_1} \times p_T^{j_2})$  [6], where  $\ell_1$  and  $\ell_2$  denote the two leptons in no particular order and  $j_1$  and  $j_2$  denote the two most energetic jets in the event. It is natural to assume that not all of the sensitivity to longitudinal scattering is encompassed in a single variable, and that better discrimination could be obtained by combining the available event information with a machine learning technique. In this paper we develop a method to use a neural network to map measurable quantities to the truth  $\cos\theta^*$  values that contain the polarization information of the two  $W$  bosons.

## II. MACHINE LEARNING MODEL

While it has become common practice in high energy physics to use multi-variate techniques to separate signal from background, to the author's knowledge multi-variate regression has not been used to directly predict underlying quantities **also not in H properties?**. Recent success with deep learning in other areas of HEP [8, 8] **???incomplete sentence**.

For the  $W^\pm W^\pm jj$  events, we use representative measurable quantities such as the transverse momentum ( $p_T$ ), pseudorapidity ( $\eta$ ) and azimuthal angle ( $\theta$ ) **you mean polar angle theta or azimuthal angle phi? I assume the latter bc. we use theta in eta already.** of the two leptons and two jets, and  $x$  and  $y$  components of the missing transverse energy ( $\cancel{E}_T^x$  and  $\cancel{E}_T^y$ ). Thus, the overall number of measurable quantities we use is 14. The goal of the multi-variate technique is then to find the best mapping from these measurable quantities to the two truth values of  $\cos\theta^*$  (one for each  $W$  boson) present in each event. We choose a multi-layer neural network with a final output layer with linear activation. The neural network was implemented with the Theano software packages [? ]. Hyper-parameters were tuned by hand, but undoubtedly could be improved. The cost function is defined as the mean error squared:

$$\mathcal{C} = \sum_{i=1}^N [(\cos\theta_{1,i}^* - N_{1,i})^2 + (\cos\theta_{2,i}^* - N_{2,i})^2] / 2N \quad (2)$$

where  $N$  is the overall number of events used,  $\cos\theta_{1/2,i}^*$  is the truth value of  $\cos\theta^*$  for each  $W$  boson with random ordering for the  $i$ -th event, and  $N_{1,2,i}$  is the value of the two neural network outputs. The stochastic gradient descent algorithm [? ] is used to find all weights and biases in the neural network that minimizes the overall cost function using a training sample.

We generate **\*\*\***  $W^\pm W^\pm jj$  events using the MADGRAPH event generator [? ] at a proton-proton center-of-mass energy of 13 TeV. The NN23101 **this is the MG internal name - use the full name?** parton distribution function [? ] is used as the default. **PS used? Pythia?** To emulate the behavior of a typical general-purpose LHC detector, these events are then passed through the detector response simulation of the ATLAS detector implemented in DELPHES [? ]. **mention jet alg/size etc. here** Events are split into three categories: 1/4 are used in a training sample, 1/4 are used for a validation test against over-training, and the remaining 1/2 are used to build templates and do sensitivity studies. A **\*\*** layer neural network with **\*\*** hidden neurons and a learning rate of **\*\*** is used.

## III. SIGNAL MODEL

To reduce the contributions from other SM processes, we apply the following generator level cuts on the  $W^\pm W^\pm jj$  sample:

- Quark  $p_T > 20$  GeV and  $|\eta| < 5$ ;
- Lepton  $p_T > 10$  GeV and  $|\eta| < 2.5$ ;
- $\Delta R_{jj} > 0.4$ ,  $\Delta R_{\ell\ell} > 0.4$  and  $\Delta R_{\ell,j} > 0.4$ ;
- Invariant mass of the two quarks  $M_{jj} > 150$  GeV.

The resulting cross section at 13 TeV is 8.4 fb, which is used to normalize the expected number of signal events.

We will first demonstrate the usefulness of deep learning networks with this general sample and then discuss the effects of cuts to reject other backgrounds as well as detector modeling effects. **so this is at truth level before delphes, and no cuts applied? Need to better define "general/default/original" here and below.**

Polarization fractions are first obtained on the default sample by fitting the two-dimensional distribution of the truth  $\cos\theta^*$  variable for each  $W$  boson. In order to fit for these polarization fractions templates must be built for "pure" polarization states. These templates are created by reweighting each event based on the truth  $\cos\theta^*$  distribution. The weight  $W_i$  for the  $i$ -th event is given by  $W_i = F_i/n_i$ , where  $n_i$  is used for the normalization and is defined as

$$n_i = \left[ \frac{3}{8} f_- (1 \mp \cos\theta_1^*)^2 + \frac{3}{8} f_+ (1 \pm \cos\theta_1^*)^2 + \frac{3}{4} f_L (1 - \cos^2\theta_1^*) \right] \times \left[ \frac{3}{8} f_- (1 \mp \cos\theta_2^*)^2 + \frac{3}{8} f_+ (1 \pm \cos\theta_2^*)^2 + \frac{3}{4} f_L (1 - \cos^2\theta_2^*) \right]. \quad (3)$$

The  $F_i$  represent the six possible polarization states for the two  $W$  bosons: Left-Left ( $--$ ), Left-Right ( $-+$ ), Right-Right ( $++$ ), Left-Longitudinal ( $-L$ ), Right-Longitudinal ( $+L$ ), or Longitudinal-Longitudinal ( $LL$ ). They are defined as

$$F_i \in \begin{pmatrix} -- = f_-^2 (1 \mp \cos\theta_1^*)^2 (1 \mp \cos\theta_2^*)^2, \\ -+ = f_- f_+ [(1 \mp \cos\theta_1^*)^2 (1 \pm \cos\theta_2^*)^2 \\ + (1 \pm \cos\theta_1^*)^2 (1 \mp \cos\theta_2^*)^2], \\ ++ = f_+^2 (1 \pm \cos\theta_1^*)^2 (1 \pm \cos\theta_2^*)^2, \\ -L = f_- f_L [(1 \mp \cos\theta_1^*)^2 (1 - \cos^2\theta_2^*) \\ + (1 - \cos^2\theta_1^*) (1 \mp \cos\theta_2^*)^2], \\ +L = f_+ f_L [(1 \pm \cos\theta_1^*)^2 (1 - \cos^2\theta_2^*) \\ + (1 - \cos^2\theta_1^*) (1 \pm \cos\theta_2^*)^2], \\ LL = f_L^2 (1 - \cos^2\theta_1^*) (1 - \cos^2\theta_2^*) \end{pmatrix}. \quad (4)$$

Since no ordering is applied to the two bosons we require that the individual polarization fractions  $f_-, f_+, f_L$  are the same for both  $W$  bosons. For reweighting the original sample  $f_-, f_+, f_L$  are take as a function of the invariant mass of the diboson system ( $M_{WW}$ ). Weights are calculated before any additional event level cuts are made, and the resulting templates are remade for each set of cuts explored. To validate the reweighting procedure, we also generate pure polarization state samples using MADSPIN and compare the obtained events kinematics with those obtained from the reweighted sample. **Does this mean you got the MG5 scripts to work and add the helicity to the lhe?** Figure 1 shows the calculated  $\cos\theta_1^*$  vs  $\cos\theta_2^*$  distribution for all six polarization states.

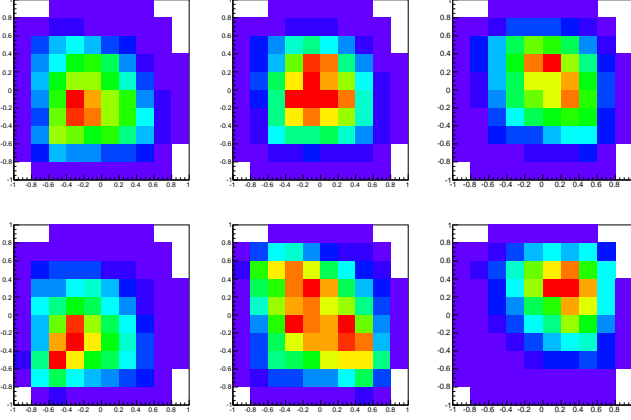


FIG. 1. Two-dimensional  $\cos\theta_1^*$  vs.  $\cos\theta_2^*$  templates after reweighting to pure polarization states which are clock-wise starting from the upper left: LO, OO, RO, LL, LR, RR. **nomenclature: L is left here, longitudinal in eq. 4? Need axis labels, larger figure...**

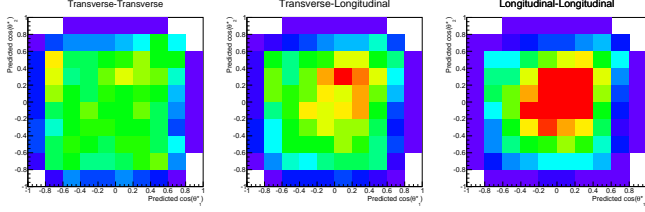


FIG. 2. Two-dimensional  $\cos\theta_1^*$  vs.  $\cos\theta_2^*$  templates after reweighting to the three polarization states  $TT$  (left),  $TL$  (middle) and  $LL$  (right).

We combine events with both  $W$  bosons transversely-polarized as “ $TT$ ” (the sum of  $--$ ,  $-+$  and  $++$  combinations), events with one  $W$  boson transversely-polarized and one  $W$  boson longitudinally-polarized as “ $TL$ ” (the sum of  $-L$  and  $+L$  combinations), and events with both  $W$  bosons longitudinally-polarized as “ $LL$ ”. This allows to better constrain the  $LL$  scattering fraction of interest, under the assumption that the relative admixture of contributions within  $TT$  and  $TL$  does not change. Figure 2 shows the calculated  $\cos\theta_1^*$  vs  $\cos\theta_2^*$  distribution for these three polarization states. **random remark: these dists seem symmetric wrt. the 45 deg bi-sector? If so, one could gain stat power by adding both halves up and using halved templates?**

Figure 3 shows the normalized  $R_{pT}$  templates for these three polarization states. The differences at large  $R_{pT}$  indicate the sensitivity of this variable to different polarization states.

#### IV. RESULTS

Having established templates for each polarization state and a distribution that is sensitive to different po-

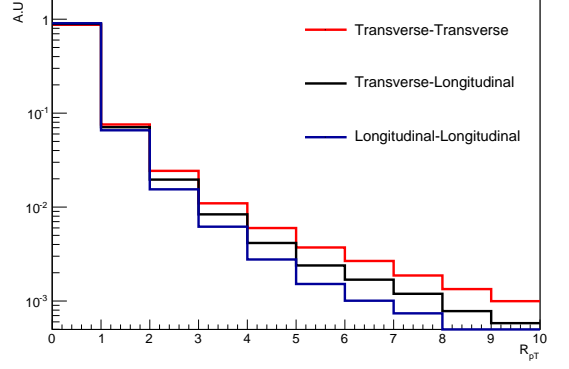


FIG. 3.  $R_{pT}$  templates for three polarization states:  $TT$ ,  $TL$  and  $LL$ . **is the legend correct? I thought LL is between TL, TT?**

larization states, all we have to do is fit the resulting calculated  $\cos\theta_1^*$  vs  $\cos\theta_2^*$  two-dimensional distribution in data to derive each polarization fraction. In actual data analysis, this would involve first selecting events to remove SM backgrounds and then subtracting predicted background from data. The effect of additional selection criteria and backgrounds is covered below, but for the case of this section we assume that MADGRAPH selection can be fitted directly to obtain sensitivities. A maximum likelihood fit is performed with the RooFit framework [? ]. Fit uncertainties are determined by randomly fluctuating data expectations within their Poisson errors and repeating the fit, and confidence intervals are derived from the toy experiments. To validate the fitting method, we also make sure the fitted values for each fraction agree with the values obtained at the truth level. **transition from truth level templates to reco level dists not clear; where has NN been used?**

The precision for all six polarization fractions as a function of the integrated luminosity are presented in Fig. 4. The corresponding precision by fitting the  $R_{pT}$  distributions are also shown for comparison. Better precision is obtained for the calculated  $\cos\theta^*$  variables, which indicates that it is a more sensitive variable to different polarization states than  $R_{pT}$ . The precision for the  $LL$  fraction is  $^{**}\%$  ( $^{**}\%$ ) for an integrated luminosity of 100 (3000)  $\text{fb}^{-1}$ , to be compared with  $^{**}\%$  ( $^{**}\%$ ) when using  $R_{pT}$ .

The precision for the three combined polarization fractions  $TT$ ,  $LT$ ,  $LL$  as a function of the integrated luminosity are presented in Fig. 5. The corresponding precision by fitting the  $R_{pT}$  distributions are also shown for comparison. As expected, better precision can be obtained by reducing the number of templates used. Transverse components can be measured with great precision, whereas separating pure longitudinal-longitudinal scattering from longitudinal-transverse scattering is challenging. However, if we fix the  $TL$  fraction to the SM prediction, we can perform a precise measurement of the  $LL$  fraction, as

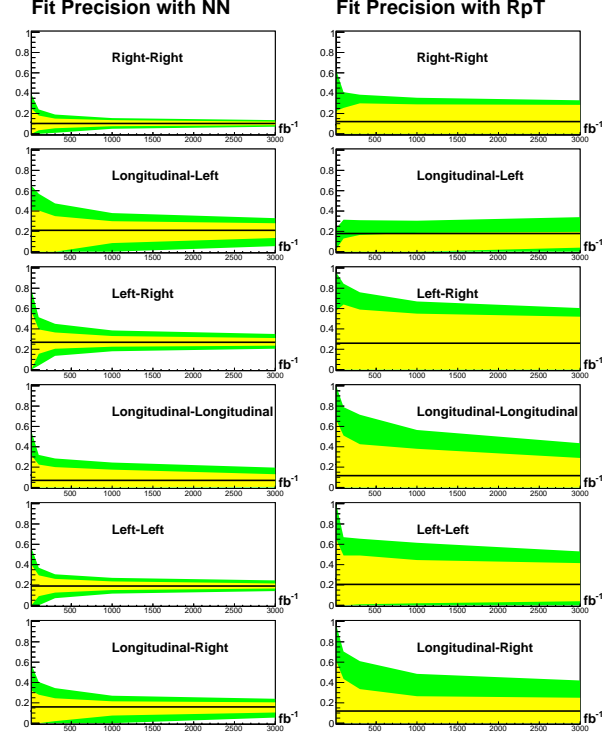


FIG. 4. 68% and 95% confidence intervals for fits with six polarization templates as a function of integrated luminosity. Fits are shown for the neural network on the left and for  $R_{pT}$  on the right.

shown in Fig. 6. In all cases the neural network output outperforms the  $R_{pT}$  variable by \*\*% or more. **fix TL to SM or use TT+LT+LL=1 ?**

While the success of this neural network at the parton level is encouraging, it is important to check if this procedure will stand up to experimental realities of finite detector resolution and non-VBS background. To reduce SM backgrounds in the loose fiducial region as defined in Sect. III, we apply similar **additional** cuts as used by the ATLAS collaboration [3] to obtain a tight fiducial region:

- Jet  $p_T > 30$  GeV;
- Lepton  $p_T > 25$  GeV;
- $\cancel{E}_T > 40$  GeV;
- $M_{jj} > 500$  GeV;
- $|\Delta Y_{jj}| > 2.4$ .

After the application of these cuts the dominant background comes from  $WZjj$  production where one lepton is not detected or not reconstructed. For the generated  $W^\pm W^\pm jj$  events, we also use PYTHIA6 for parton shower and hadronization simulation and then pass these events through the DELPHES package (using the CMS simulation card) [?] to simulate the detector response of

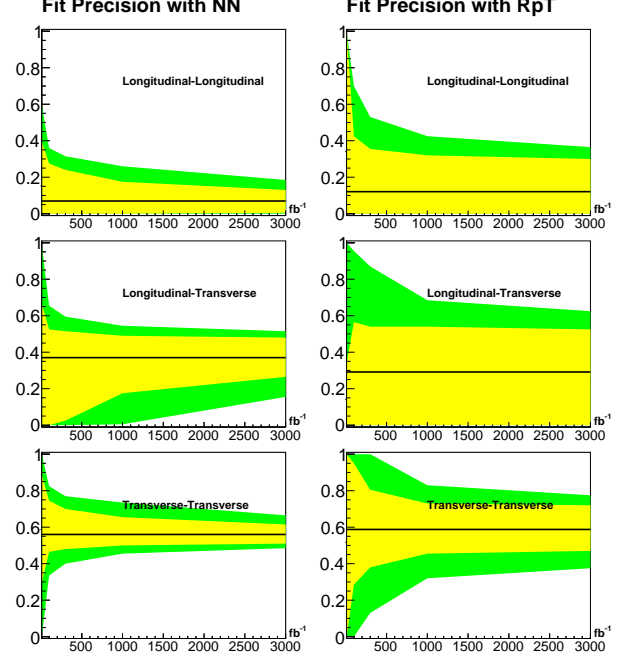


FIG. 5. 68% and 95% confidence intervals for fits with three polarization templates as a function of integrated luminosity. Fits are shown for the neural network on the left and for  $R_{pT}$  on the right.

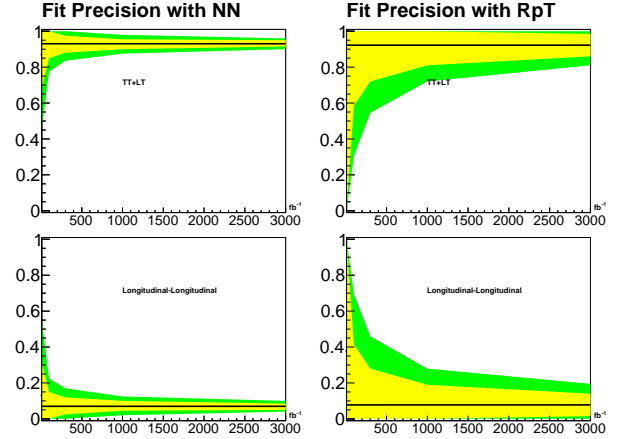


FIG. 6. 68% and 95% confidence intervals for fits with two polarization templates as a function of integrated luminosity. Fits are shown for the neural network on the left and for  $R_{pT}$  on the right. **if you use TT+LT+LL=1 you also end up with two independent pars only to fit...**

a general-purpose particle detector at the LHC **repeat from above, rm once. Maybe easier to follow if first parton level studies are shown and then delphes?** We define the loose and tight fiducial regions at both the parton level and also at the DELPHES level. Table I shows the extracted limits on TT, TL and LL fractions for loose and tight fiducial regions defined at the parton level and at the DELPHES level. Table II shows

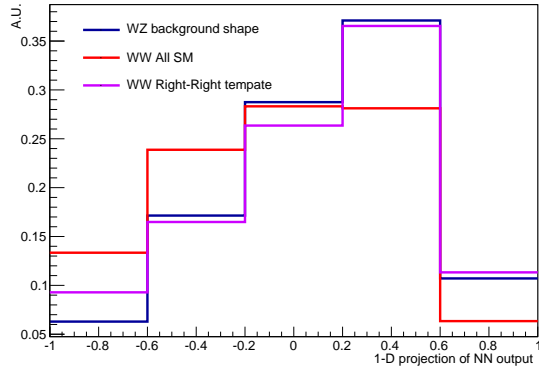


FIG. 7. Signal and background shapes for the calculated  $\cos \theta^*$ .

the corresponding numbers on TT+TL and LL fractions. An integrated luminosity of  $** \text{ fb}^{-1}$  is assumed.

Figure 7 shows the calculated **I removed “calculated” a couple times now, but you likely want to imply with it that it stems from the NN? Need to come up with proper labeling  $\cos \theta^*$  distribution for the dominant  $WZ$  background,  $++$  and  $LL$  figure caption/legend contradict text:  $++$  vs.  $RR$ , AllSM vs.  $??$  components of the  $W^\pm W^\pm jj$  events. It can be seen that the calculated  $\cos \theta^*$  distribution for the  $WZ$  background closely resembles that of the  $++$  template, and it will be important to subtract the  $WZ$  contribution before the actual fitting.**

Fiducial region	TT		TL		LL	
	LL	UL	LL	UL	LL	UL
Loose (parton level)	0.51	0.62	0.27	0.48	0.01	0.13
Tight (parton level)	0.47	0.63	0.19	0.52	0.0	0.19
Loose (DELPHES level)	0.48	0.65	0.16	0.52	0.0	0.21
Tight (DELPHES level)	0.44	0.66	0.08	0.56	0.0	0.27

TABLE I. Lower Limits (LL) and Upper Limits (UL) **which CL?** on the TT, TL, and LL fractions for loose and tight fiducial regions defined at the parton level and at the DELPHES level. **why does tight not give better limits?**

Fiducial region	TT+TL		LL	
	LL	UL	LL	UL
Loose (parton level)	0.92	0.95	0.05	0.09
Tight (parton level)	0.89	0.95	0.05	0.11
Loose (DELPHES level)	0.9	0.95	0.05	0.11
Tight (DELPHES level)	0.87	0.95	0.05	0.13

TABLE II. Lower Limits (LL) and Upper Limits (UL) on the TT+TL and LL fractions for loose and tight fiducial regions defined at the parton level and at the DELPHES level. **see above table caption comments**

## V. CONCLUSIONS

We present a method to determine the  $WW$  polarization fractions in  $W^\pm W^\pm jj$  events by using a deep machine learning technique. This method allows to recover the charged lepton angular distributions in the  $W$  boson rest frame from measurable event kinematics. We compare the results obtained from this method and from other traditional methods to illustrate the gain in sensitivity with our method. Cuts to reject backgrounds as well as detector smearing reduces the sensitivity as expected, but the method remains a useful tool for the study of polarization fractions in VBS.

- [1] G. Aad *et al.* [ATLAS Collaboration], Phys. Lett. B **716**, 1 (2012) [arXiv:1207.7214 [hep-ex]].
- [2] S. Chatrchyan *et al.* [CMS Collaboration], Phys. Lett. B **716**, 30 (2012) [arXiv:1207.7235 [hep-ex]].
- [3] G. Aad *et al.* [ATLAS Collaboration], Phys. Rev. Lett. **113**, no. 14, 141803 (2014) [arXiv:1405.6241 [hep-ex]].
- [4] V. Khachatryan *et al.* [CMS Collaboration], Phys. Rev. Lett. **114**, no. 5, 051801 (2015) [arXiv:1410.6315 [hep-ex]].
- [5] T. Han, D. Krohn, L. T. Wang and W. Zhu, JHEP **1003**, 082 (2010) [arXiv:0911.3656 [hep-ph]].
- [6] K. Doroba, J. Kalinowski, J. Kuczmarski, S. Pokorski, J. Rosiek, M. Szleper and S. Tkaczyk, Phys. Rev. D **86**, 036011 (2012) [arXiv:1201.2768 [hep-ph]].
- [7] P. Baldi, P. Sadowski and D. Whiteson, Nature Commun. **5**, 4308 (2014) [arXiv:1402.4735 [hep-ph]].
- [8] P. Baldi, P. Sadowski and D. Whiteson, Phys. Rev. Lett. **114**, no. 11, 111801 (2015) [arXiv:1410.3469 [hep-ph]].